

Visible imaging of the diagnostic neutral beam on TFTR

G. Schilling, S. S. Medley, and S. J. Zweben
Princeton Plasma Physics Laboratory, Princeton, New Jersey 08543

(Presented on 8 May 1990)

An attempt was made to image the 2-D spatial patterns of the edge density turbulence of the Tokamak Fusion Test Reactor (TFTR) by using the visible light emission from an injected diagnostic neutral beam (DNB). A clear image of the 12 cm \times 20 cm DNB "sheet beam" was obtained using the Doppler-shifted line emission at 584.9 ± 0.5 nm (2.7 nm blue shifted) from the neutral helium beam with a 2 ms exposure time. Although the signal level was too low to observe the edge density turbulence, potential improvements are described which could improve the sensitivity enough to obtain an image on the desired 10 μ s timescale.

I. INTRODUCTION

It seems to be widely recognized that full 2-D (or even 3-D) imaging is necessary in order to fully characterize ordinary fluid turbulence.¹ In fact, the results of 2-D imaging studies often disclose "coherent" structures within fluid turbulence which would not be apparent in 0-D time series or 1-D cross-correlation studies.^{2,3} This paper describes an attempt to form a 2-D image suitable for characterizing tokamak edge density turbulence.

The general requirements for such 2-D plasma imaging can be set by previous observations of tokamak density fluctuations.⁴ For large tokamaks such as the Tokamak Fusion Test Reactor (TFTR), the spatial scale lengths of interest are in the range 1–10 cm, the timescales of interest are 10–100 μ s (with the larger timescale for the larger space scale), and the relative density fluctuation levels in the range <1% at the plasma center to \approx 10% at the plasma edge.

Previous 2-D Langmuir probe⁵ and H_α emission⁶ studies of the relatively large-level edge density turbulence have shown it to be composed of toroidally elongated "filaments" which seem to move irregularly in the plane perpendicular to the toroidal field. The present paper describes an attempt at a new technique which could potentially extend these observations substantially. However, the results obtained so far are limited by the relatively low signal levels of this preliminary experiment, as discussed in Sec. IV.

II. METHOD

An idealized schematic view of the present imaging technique is shown in Fig. 1. The idea is to inject a source of neutral atoms in a 2-D "sheet beam" which itself emits light and which can be viewed with a sensitive camera. Plasma density fluctuations will produce local variations in the atomic excitation and spectral line emissivity of the beam atoms,⁷ and so an image of the 2-D plasma density fluctuation pattern could be obtained if the camera is gated on the appropriate timescale. This technique is quite analogous to fluid experiments which use a fluorescent dye excited by a 2-D laser sheet beam to determine the internal structure of turbulent jets.²

The actual geometry used for the present experiment is shown in Fig. 2. The neutral atoms are injected radially into

the plasma by the TFTR diagnostic neutral beam (DNB). The beam emission is viewed through a remotely controllable periscope (part of the plasma TV system) from a distance of \approx 7 m across the plasma with an externally gated single-microchannel-plate intensified video camera. Note that this geometry was far from ideal, due mainly to the large distance between the DNB and the camera and the undesirably small angle between the sightline and the beam direction (\approx 30°).

The DNB itself⁸ injected either hydrogen or helium beams into the plasma outer midplane. The beam energy was typically 50–60 keV, the injected neutral current was \approx 5 A, and the beam size (FWHM) at the plasma edge was about 12 cm (toroidally) by 20 cm (vertically). The beamwidth could have been reduced to \approx 1 cm for better spatial resolution with plates within the beam box; however, a proportional loss of beam current would have occurred.

The periscope system⁹ viewed the DNB region from the midplane with relatively "slow" $f/8$ optics and a transmission of \approx 40% in visible light. The main advantage of this periscope was its remotely controllable orientation, magnification, focus, iris, and filter wheel.

A Xybion ISG-250 intensified CCD video camera¹⁰ was attached to the periscope in the neutron-shielded TFTR basement. Its pixel format was 380 horizontal \times 240 vertical, its sensitivity was better than 1×10^{-7} foot

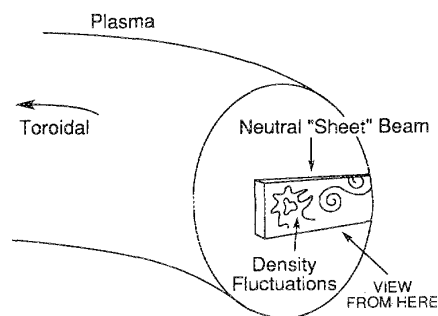


FIG. 1. Schematic view of the imaging of the diagnostic neutral beam (DNB) emission. The DNB enters radially as a vertically elongated "sheet" beam, and local plasma density fluctuations cause variations in the beam's light emission (illustrated very schematically). For good spatial resolution the beam emission is best viewed nearly perpendicularly to the beam plane.

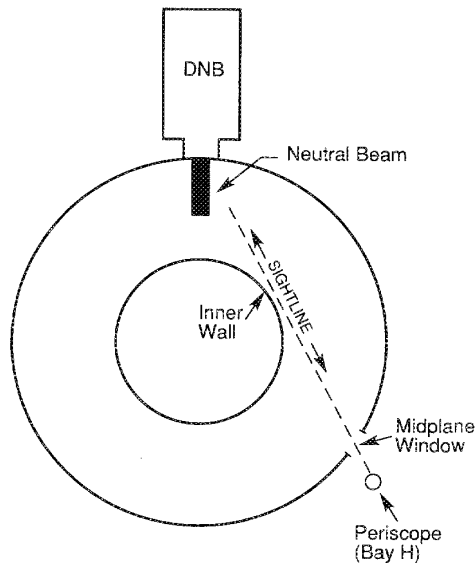


FIG. 2. Geometry of the present attempt at beam imaging. The view is at an angle of 30° to the beam direction, and from a distance of about 7 m from the DNB. The view of the DNB emission is also partially obstructed by the inner wall of the tokamak.

candles (see below), and its microchannel plate could be gated (by computer) from $<10 \mu\text{s}$ to 16 ms exposure per frame. This camera produced one frame every 32 ms, so that the high-frequency temporal structure of the turbulence could not be followed at all. Note that this camera was about ten times more sensitive than the one used previously to image turbulent H_α fluctuations near the inner wall of TFTR.⁶

Several optical interference filters were stationed in the periscope filter wheel in front of the camera faceplate. The spectral line used in the present experiment was the 587.6 nm line of neutral helium. Since light from the beam emission is Doppler shifted when viewing along the beam direction, the filter was chosen to be 584.9 ± 0.5 for the helium beam, corresponding to a viewing angle of 30° and beam energy of 50 keV.

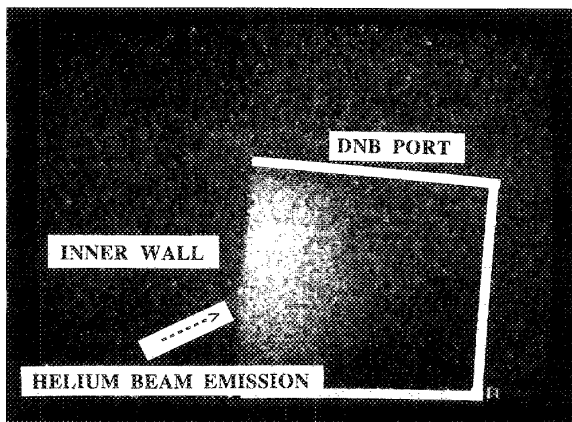


FIG. 3. Image of the helium beam emission from a TFTR discharge (shot #45213). This light is observed only during the DNB injection time, and only at the DNB port region. However, the exposure time of 2 ms was too long to observe the expected edge density turbulence.

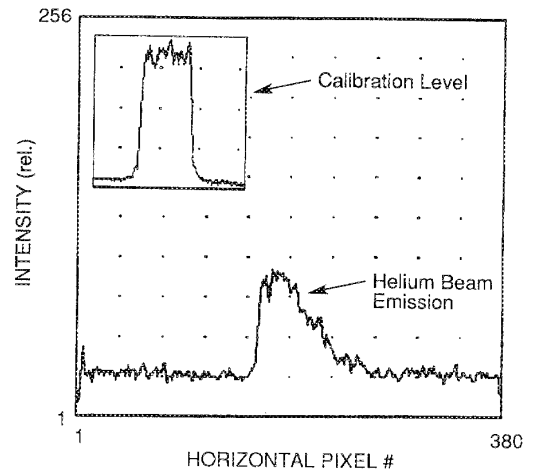


FIG. 4. Digitization of the light emission from the image of Fig. 3. The bottom trace is from a 3-cm-high vertical slice at the center of the beam emission region (i.e., averaged over 15 vertical lines). The calibration level shown in the corner is from a bench-top 600 nm source viewed by the same camera at the same exposure time and $f\#$, showing that the fluctuation level observed in the helium beam image is also present in the calibration source.

III. RESULTS

The best images of neutral beam emission were all similar to the single frame shown in Fig. 3, which was obtained with ≈ 5 A of 60 keV helium beam injection at a 2 ms exposure time (in a 2 MA ohmic discharge). The light in this region turned on (and off) within one frame (32 ms) of the DNB turn-on (and turn-off), and was approximately constant during the 300 ms DNB duration, as expected. This light was also located only in the region near the DNB, as indicated by the boundaries of the DNB port in Fig. 3. Note that the sharp left-hand boundary of the emissive region is the obstructing inner wall of the vacuum vessel (see Fig. 2).

Clearly such images are not yet useful for studying plasma density fluctuations of the magnitude and the timescale mentioned above. The exposure timescale is approximately 100 times too long, and the spatial averaging due to the 12 cm beamwidth (toroidally) and 30° viewing angle (i.e., ≈ 24 cm radially) is about ten times too large to resolve few-cm-sized fluctuations. The remainder of this section attempts to quantify the signal and noise levels of this image in order to help motivate possible improvements to this system (Sec. IV).

A digitization of a horizontally oriented slice of Fig. 3 is shown in Fig. 4. This particular slice averages over a vertical distance of about 3 cm near the center of the DNB, or about 15 vertical lines in the digitized image. The peak signal is about 2.5 times the local background and about 30% of the maximum video intensity level (digitized to 8 bits).

An absolutely calibrated bench-top optical source¹¹ was used to calibrate the camera. This was done by setting the camera to the same exposure time (2 ms) and using the same $f\#$ ($f/8$) as in the experiment, and determining the flux of light (at 600 ± 3.5 nm) which reproduces the signal level observed in Fig. 4. The result was that a source in-

tensity of 1.6×10^{-7} W/(cm² str) produced approximately the same signal level as the helium beam emission, as shown in the insert of Fig. 4. Thus the brightness of the helium beam emission in the experiment was $\approx 4 \times 10^{-7}$ W/(cm² str), after accounting for the 40% transmission of the periscope itself.⁹ This agrees fairly well with an independent measurement of 8×10^{-7} W/cm² str for the same TFTR helium beam.¹²

This result can be used to form a rough estimate of the number of 587.6 nm helium photons produced per injected neutral helium atom. The area of the helium source as seen by the camera was ≈ 600 cm², and the photons were emitted into 4π str, so that the total number of photons emitted by the beam was $\approx 10^{18}$ photons/s. The total injected beam atom flux was $\approx 3 \times 10^{19}$ atoms/s; therefore, the number of helium photons per injected helium atom was ≈ 0.03 .

The same calibration can be used to estimate the fluctuation level expected from photon statistics in the data of Fig. 3. For a source of brightness 4×10^{-7} W/(cm² s) of 600 nm photons into an $f/8$ system of $\approx 10^{-2}$ str exposed for 2 ms/frame, the photon flux into the camera was $\approx 10^9$ photons/(frame cm²), where the area now refers to the size of the image on the CCD of a 1 cm² area of the source. Since 1 cm² of calibration source area was imaged onto ≈ 250 pixels of the CCD, and the pixel size was $11 \mu\text{m} \times 13 \mu\text{m}$, the number of photons per pixel per frame, after taking into account the photocathode quantum efficiency of about 0.06 and the active area of the pixels (65%), was about 100 photons/(pixel frame).

This result can be compared with the observed fluctuation level in the digitized signal of Fig. 4, where each horizontal pixel averages over 15 vertical pixels. The expected fluctuation level from photon statistics is $1/\sqrt{(100 \times 15)} \approx 3\%$, while the observed fluctuation level in the helium signal and also the calibration signal (inset) is roughly 2–5% rms. Thus it is plausible that the fluctuations so far observed in the helium beam emission are simply due to photon counting statistics.

IV. POSSIBLE IMPROVEMENTS

This diagnostic can be improved in several possible ways:

(1) Replacing the rather inefficient $f/8$ optical system of the standard TFTR periscope with a customized $f/1.5$ system will improve the photon flux by $(8/1.5)^2 \approx 30$. An attempt in this direction has already been made on TFTR using a coherent fiber bundle to couple plasma images from a large lens near the vessel to a remote camera.¹³

(2) Decreasing the distance between the first lens and the beam by up to a factor of 3 (i.e., from 7 to 2 m) could further increase the photon flux (per unit beam area) by up to a factor of 10.

(3) Increasing the neutral atom flux of the beam, which can potentially be increased a factor of 5 by replacing the existing ion source with a larger source utilizing spherically focusing grids.

(4) Finding an atom which produces more photons per atom than does this line of helium. The ideal beam would have good penetration, slow beam velocity, a short excited state lifetime, and a large excitation cross section.

Possible beam species include all the noble gases, although the excitation of visible lines tends to decrease for higher Z atoms.

The first two optical improvements could increase the photon flux per unit beam area by a factor of 200, thus allowing an image of the quality of Fig. 3 (but taken at an angle of $\approx 60^\circ$ to the beam) to be obtained at an exposure time of about 10 μs . Such an image might show some evidence of large-scale (≈ 5 cm), large-amplitude ($\approx 10\%$) edge density fluctuations such as were seen previously in wall-recycled hydrogen light.⁶

We should also note some aspects of this diagnostic which cannot be so easily improved:

(5) Improvements in camera sensitivity are not useful beyond the present level ($\approx 10^{-7}$ foot candles sensitivity at the camera faceplate), since the signal-to-noise level already seems to be set by photon-counting statistics.

(6) Nonuniformities in the CCD array itself limit the ability of the video system to distinguish small spatial variations in intensity, as observed by a reproducible 1–2% frame-to-frame spatial variation in white fields with arbitrarily large light levels (however, these nonuniformities can be corrected for with appropriate image processing).

(7) Improvements in radial spatial resolution are limited by the lifetime of the excited atomic state, which for this helium line is 10 ns,¹² which results in a spatial “smearing” over about 1–2 cm for beam ion speeds of $1\text{--}2 \times 10^8$ cm/s. Note also that the long parallel wavelength of these fluctuations makes the effect of toroidal plasma rotation on the spatial resolution relatively weak, e.g., a toroidal rotation speed of 10^7 cm/s will smear the local spatial structure only after about 100 μs .

In summary, we could expect to obtain a useful edge fluctuation imaging system for TFTR with some relatively simple improvements in the optical collection efficiency. However, the present video system seems to be limited to measuring fluctuation levels of $> 5\%$, so would not be appropriate for measuring the $< 1\%$ density fluctuations in the plasma interior.

ACKNOWLEDGMENTS

We thank D. W. Johnson, J. Montague, S. Hayes, E. Synakowski, B. Stratton, K. M. Young, and M. Zarnstorff for help with and discussions about this project. This work was supported by DOE contract DE-AE02-76-CHO3073.

¹J. A. Ferre, J. C. Mumford, A. M. Savill, and F. Giralt, *J. Fluid Mech.* **210**, 371 (1990).

²A. K. M. F. Hussain, *Phys. Fluids* **26**, 2816 (1983).

³K. W. Schwartz, *Phys. Rev. Lett.* **64**, 415 (1990).

⁴P. C. Liewer, *Nucl. Fusion* **25**, 543 (1987).

⁵S. J. Zweben and R. W. Gould, *Nucl. Fus.* **25**, 171 (1985).

⁶S. J. Zweben and S. S. Medley, *Phys. Fluids B* **1**, 2058 (1989).

⁷R. Fonck (this conference).

⁸G. Schilling, T. A. Kozub, S. S. Medley, and K. M. Young, *Rev. Sci. Instrum.* **57**, 2060 (1986).

⁹S. S. Medley, D. L. Dimok, S. Hayes, D. Long, J. L. Lowrance, V. Mastrocola, G. Renda, M. Ulrickson, and K. M. Young, *Rev. Sci. Instrum.* **56**, 1873 (1985).

¹⁰Obtained from Xyberon Electronic Systems Inc., San Diego, CA.

¹¹Optronic Laboratories Model 420.

¹²F. Levinton (private communication).

¹³D. W. Johnson (private communication).